

Free-radical reactions of the tris-dioximate clathrochelates: synthesis and X-ray structure of the first cyclohexyl-substituted monoribbed-functionalized macrobicyclic iron(II) complex*

A. B. Burdukov,^{a*} M. A. Vershinin,^a N. V. Pervukhina,^a S. G. Kozlova,^a I. V. El'tsov,^b and Ya. Z. Voloshin^c

^aA. V. Nikolaev Institute of Inorganic Chemistry, Siberian Branch of the Russian Academy of Sciences, 3 prosp. Lavrent'eva, 630090 Novosibirsk, Russian Federation.

Fax: +7 (383) 330 9489. E-mail: lsc@niic.nsc.ru

^bNovosibirsk State University,

2 ul. Pirogova, Novosibirsk, Russian Federation.

Fax: +7 (383) 363 4183. E-mail: eiv@fen.nsu.ru

^cA. N. Nesmeyanov Institute of Organoelement Compounds, Russian Academy of Sciences, 28 ul. Vavilova, 119991 Moscow, Russian Federation.

Fax: +7 (499) 135 5085. E-mail: voloshin@ineos.ac.ru

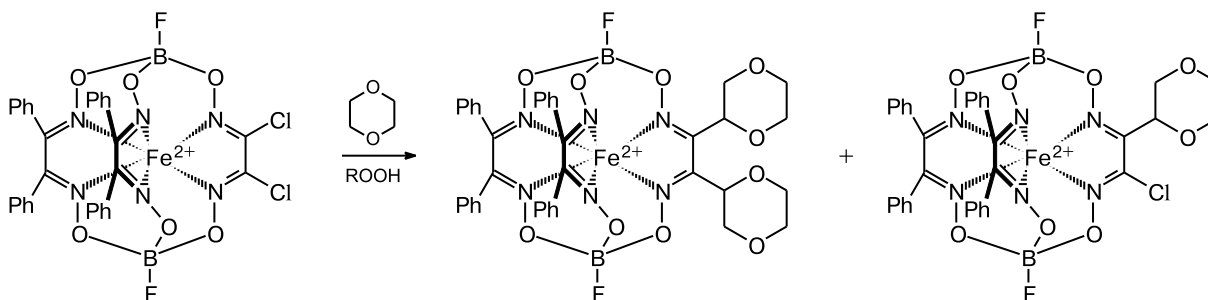
Quantum chemical calculations were performed at the DFT level for the boron-capped dichloro-substituted tris-dioximate iron(II) clathrochelate and cyclohexane and 1,4-dioxane radicals. The 1,4-dioxane and cyclohexane radicals are nucleophiles towards the macrobicyclic precursor studied. The reaction of this clathrochelate with cyclohexane in the presence of a free-radical initiator resulted in substitution of a chlorine atom by a cyclohexyl fragment. The compound obtained was characterized by elemental analysis, IR spectroscopy, ¹H and ¹³C{¹H} NMR, and single-crystal X-ray diffraction data.

Key words: clathrochelates, reactions of coordinated ligands, free-radical reactions, quantum chemical calculations.

Reactive macrobicyclic transition metals tris-dioximates are promising molecular platforms for the synthesis of polyfunctional and polytopic systems with desired properties.¹ In the most cases, ribbed functionalization of clathrochelates was performed by the substitution of reactive halogen atoms in their chelating α -dioximate fragments under the action of various nucleophiles^{2–9} and using the *in situ* generation of nucleophilic clathrochelate anions by the deprotonation of the substituents in these fragments.^{10,11}

We have recently discovered the free-radical substitution of the chlorine atoms in the ribbed fragment of the iron(II) dichloroclathrochelate $\text{FeBd}_2(\text{Cl}_2\text{Gm})(\text{BF})_2$ (where Bd^{2-} and $\text{Cl}_2\text{Gm}^{2-}$ are the α -benzylidioxime and dichloroglyoxime dianions, respectively) under the action of 1,4-dioxane radical derivatives (Scheme 1).¹² In this work, we performed the quantum chemical calculation of the clathrochelate precursor and 1,4-dioxane and cyclohexane radicals, which showed their similar reactivity towards this

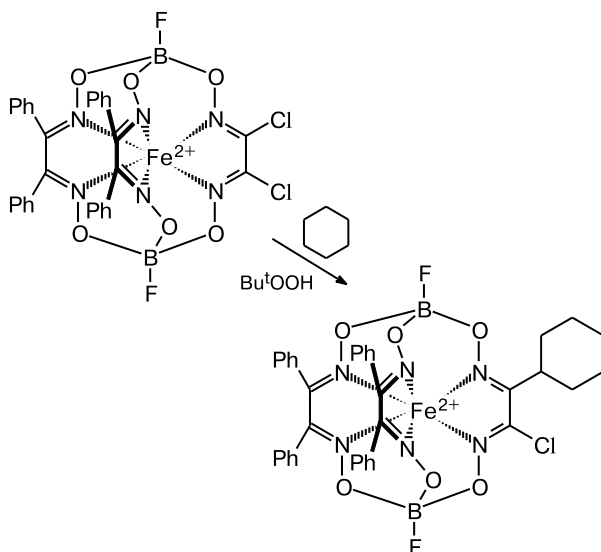
Scheme 1



* Dedicated to Academician of the Russian Academy of Sciences R. Z. Sagdeev on the occasion of his 70th birthday.

macrobicycle, in order to interpret the reaction mechanism. This made it possible to directly carry out the substitution of the chlorine atom in the ribbed chelating fragment of clathrochelate $\text{FeBd}_2(\text{Cl}_2\text{Gm})(\text{BF})_2$ by the cyclohexyl radical using *tert*-butyl hydroperoxide as a free-radical initiator (Scheme 2). The synthesized macrobicyclic complex was characterized by elemental analysis data, IR spectra, ^1H and ^{13}C NMR spectra, and X-ray diffraction analysis.

Scheme 2



Results and Discussion

The reactivity of free radicals towards double bonds depends substantially on the energy of the molecular orbital of the unpaired electron of the free radical (singly occupied molecular orbital, SOMO) and the energies of the highest occupied (HOMO) and lowest unoccupied (LUMO) molecular orbitals of the unsaturated substrate.¹³ The majority of carbon-centered radicals are nucleophilic when adding to double bonds; *i.e.*, the transition state is determined by the interaction of the SOMO of the radical and the LUMO of the substrate. The linear correlation between the rate of radical addition to the $\text{C}=\text{C}$ double bond and the LUMO energy of alkene has been previously reported.¹⁴ The SOMO energies of the $\text{C}_4\text{H}_7\text{O}_2^\cdot$ and $\text{C}_6\text{H}_{11}^\cdot$ radicals calculated by us are close, being -4.7 and -4.8 eV, respectively. The general view of their molecular orbitals are presented in Fig. 1. The highest occupied molecular orbital of clathrochelate $\text{FeBd}_2(\text{Cl}_2\text{Gm})(\text{BF})_2$ has a noticeably lower energy (-6.4 eV) than the above-mentioned SOMO of the radicals, and the LUMO energy of the macrocyclic precursor is -2.6 eV. Thus, the difference in energies of the HOMO and LUMO of this clathrochelate

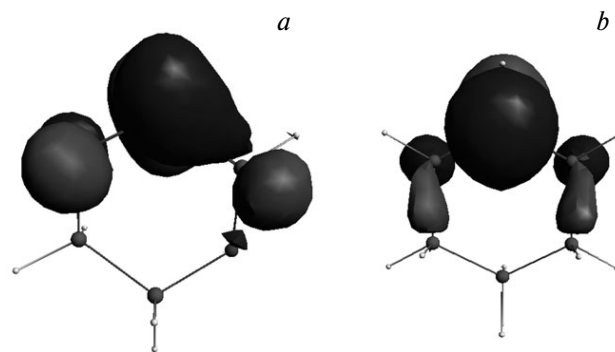


Fig. 1. Singly occupied molecular orbitals (SOMO) of the 1,4-dioxanyl (a) and cyclohexyl (b) radicals. The boundary value of the isosurface of the SOMO is 0.05.

is approximately 4 eV, which is appreciably lower than that in alkenes (~ 13 eV),¹⁴ and the SOMO of the $\text{C}_4\text{H}_7\text{O}_2^\cdot$ and $\text{C}_6\text{H}_{11}^\cdot$ radicals lies approximately in the middle between the HOMO and LUMO of the macrobicyclic polyazomethine substrate. It was shown in a series of theoretical calculations that the position of frontier molecular orbitals can substantially depend on the quantum chemical method used and chosen electron density functionals and basis sets.¹⁵ As a result, the obtained calculated values of energies do not allow one to unambiguously determine the nature of the transition state. Therefore, to elucidate the mechanism of the reaction of the radicals with clathrochelate $\text{FeBd}_2(\text{Cl}_2\text{Gm})(\text{BF})_2$, we used approaches based on the topological methods.^{16–19} The isosurfaces of the ELF functions of the radicals for electrons in the state \uparrow (ELF_A) and in the state \downarrow (ELF_B) are presented in Figs 2 and 3. According to the interpretation¹⁷ of the ELF function for the radical systems, the unpaired electron in the $\text{C}_4\text{H}_7\text{O}_2^\cdot$ and $\text{C}_6\text{H}_{11}^\cdot$ radicals is predominantly located on the carbon atoms. The calculation of the charges on the atoms by the Bader method showed that the carbon atom of the azomethine fragment of the clathrochelate has an effective positive charge of $+0.61$ e (Fig. 4), which agrees with the possibility of its attack by the radical center of 1,4-dioxan-2-yl (see Fig. 2). Thus, in the reaction studied earlier¹² (see Scheme 1) this radical exhibits the nucleophilic properties. According to the quantum chemical calculation data, the cyclohexyl radical should manifest a similar reactivity due to an analogous nature of the radical center (see Fig. 3) and almost the same energy of the SOMO.

Indeed, refluxing a solution of the clathrochelate precursor $\text{FeBd}_2(\text{Cl}_2\text{Gm})(\text{BF})_2$ in benzene containing 7% cyclohexane (v/v) in the presence of the free-radical initiator *tert*-butyl hydroperoxide resulted in the formation of the macrobicyclic complex $\text{FeBd}_2(\text{Cl}(\text{C}_6\text{H}_{11})\text{Gm})(\text{BF})_2$ in 60% yield (see Scheme 2).

It should be mentioned that *tert*-butyl hydroperoxide is a "slow" initiator: the experimentally measured rate constant

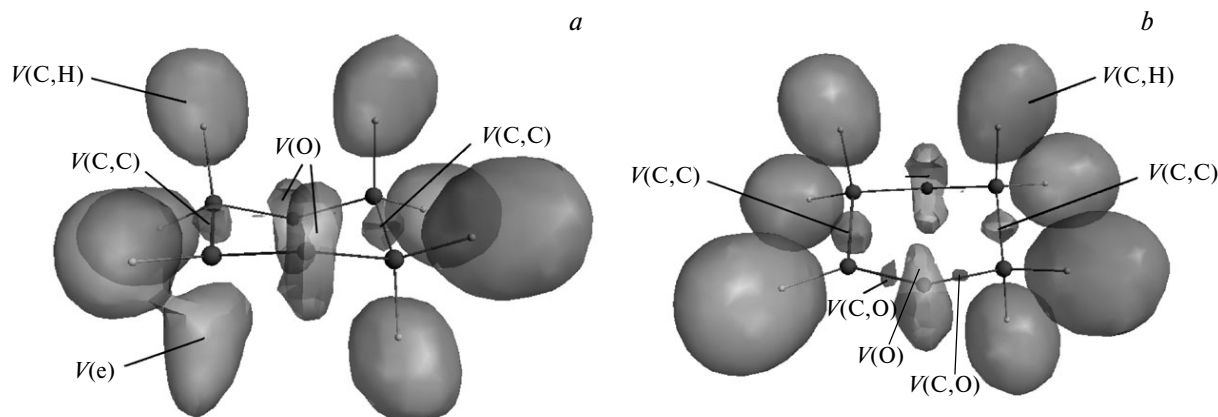


Fig. 2. Isosurfaces of the functions ELF_A with a boundary value of 0.84 (a) and ELF_B with a boundary value of 0.84 (b) for the 1,4-dioxanyl radical: $V(O)$ is the monosynaptic basin (lone electron pairs of the oxygen atom); $V(C,C)$ and $V(C,O)$ are the disynaptic basins visualizing the covalent and polar C—C and C—O bonds; $V(C,H)$ are the disynaptic protonated basins representing the C—H covalent bonds; and $V(e)$ is the basin indicating the unpaired electron localization.

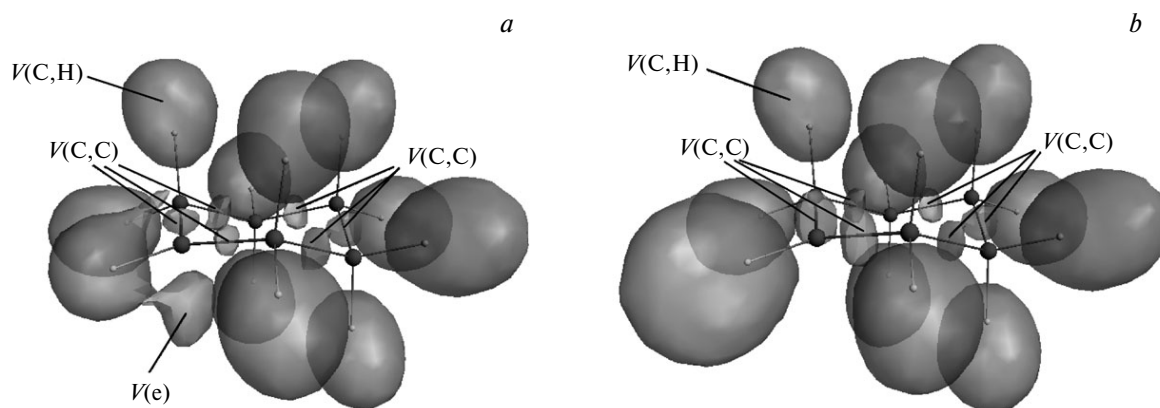


Fig. 3. Isosurfaces of the functions ELF_A with a boundary value of 0.84 (a) and ELF_B with a boundary value of 0.84 (b) for the cyclohexyl radical: $V(C,C)$ are the disynaptic basins visualizing the covalent C—C bonds; $V(C,H)$ are the disynaptic protonated basins representing the C—H covalent bonds; and $V(e)$ is the basin indicating the unpaired electron localization.

of its decomposition in benzene at 130 °C is $3 \cdot 10^{-7} \text{ s}^{-1}$ ($E_a = 138 \text{ kJ mol}^{-1}$).²⁰ Thus, at 80 °C the decomposition rate of *tert*-butyl hydroperoxide becomes negligible and it cannot act as an initiator. However, in the presence of transition metal salts, the decomposition of hydroperoxides can considerably accelerate.²⁰ The estimation of the kinetics of *tert*-butyl hydroperoxide decomposition by ¹³C NMR spectroscopy using a known procedure²¹ showed that the rate of the reaction increased sharply in the presence of the clathrocholate precursor $\text{FeBd}_2(\text{Cl}_2\text{Gm})(\text{BF})_2$ ($T_{1/2}$ is 16 h and 30 min, respectively). The nature of the observed phenomenon requires the additional study; possibly, this effect is somewhat similar to the known Fenton reaction.²²

The molecular and crystal structures of the clathrocholate $\text{FeBd}_2(\text{Cl}(\text{C}_6\text{H}_{11})\text{Gm})(\text{BF})_2$ (see Fig. 5) were established by X-ray diffraction. This complex crystallizes from a dichloromethane—hexane mixture with one di-

chloromethane molecule. The encapsulated iron(II) ion has the distorted trigonal prismatic N_6 -environment characteristic of the boron-containing tris-dioximate transition metal clathrochelates: its geometry is intermediate between the trigonal prism (distortion angle $\varphi = 0^\circ$) and the trigonal antiprism ($\varphi = 60^\circ$); the φ angle is 25.1° . The Fe—N distances in this coordination polyhedron range from 1.902 to 1.911 Å, and its height is 2.32 Å. Other bond lengths and bond angles in the clathrocholate framework have usual values. The cyclohexyl ribbed substituent has a chair conformation; the length of the C—C bond between the C(31) carbon atom of this substituent and the azomethine C(30) atom is 1.515(7) Å. A substantial variation of the C—C bond lengths in the six-membered alicyclic substituent (1.45–1.57 Å) is observed with the retention of the bond angles, whose values (106–112 and 117°) are close to the tetrahedral ones. The highest deviation from the tetrahedral value (bond angle 117°) is observed for the

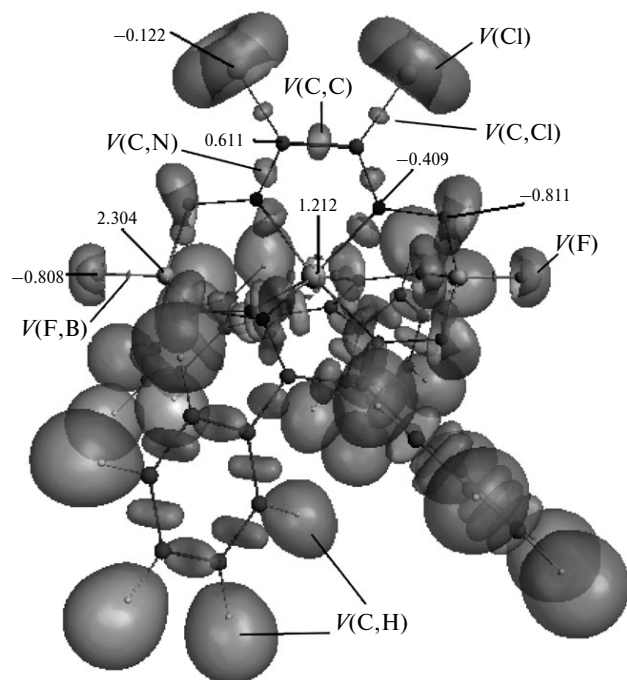


Fig. 4. Isosurface of the ELF functions with a boundary isosurface value of 0.84 for clathrochelate $\text{FeBd}_2(\text{Cl}_2\text{Gm})(\text{BF})_2$: $V(\text{C},\text{C})$, $V(\text{C},\text{Cl})$, $V(\text{C},\text{N})$, and $V(\text{F},\text{B})$ are the disynaptic basins visualizing the covalent bonds between the atoms C—C, C—Cl, C—N, and F—B; $V(\text{C},\text{H})$ are the disynaptic protonated basins representing the covalent binding between the hydrogen and carbon atoms. The numerical values of the charges on the atoms calculated using the Bader method are also presented.

carbon atom of the clathrochelate framework bound to the ribbed fragment.

The crystal of $\text{FeBd}_2(\text{Cl}(\text{C}_6\text{H}_{11})\text{Gm})(\text{BF})_2 \cdot \text{CH}_2\text{Cl}_2$ has shortened intermolecular contacts $\text{F} \cdots \text{H}_{\text{C}_6\text{H}_5}$ ($r_i = 2.54 \text{ \AA}$),

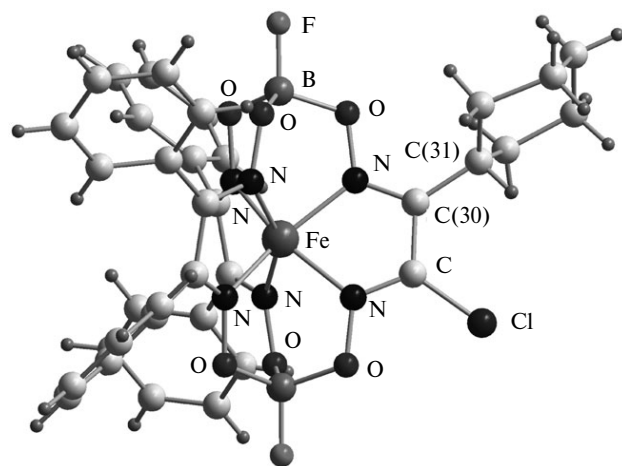


Fig. 5. Molecular structure of clathrochelate $\text{FeBd}_2(\text{Cl}(\text{C}_6\text{H}_{11})\text{Gm})(\text{BF})_2$.

$\text{F} \cdots \text{H}_{\text{CH}_2\text{Cl}_2}$ ($r_i = 2.49 \text{ \AA}$) and $\text{O} \cdots \text{H}_{\text{CH}_2\text{Cl}_2}$ ($r_i = 2.50 \text{ \AA}$), which can be considered as weak hydrogen bonds.

Thus, we found that the free-radical substitution of the chlorine atoms in the dichloro-substituted iron(II) clathrochelate is not restricted to cyclic ethers¹² and can be carried out in the case of other similar in energy radical particles (in particular, the cyclohexane radical). The radical derivatives of 1,4-dioxane and cyclohexane were shown to be nucleophilic towards this macrobicyclic precursor. The cyclohexyl-substituted monoribbed-functionalized macrobicyclic iron(II) complex has been synthesized for the first time and structurally characterized.

Experimental

The clathrochelate precursor $\text{FeBd}_2(\text{Cl}_2\text{Gm})(\text{BF})_2$ was synthesized according to a described procedure.²³ Prior to use benzene was washed with sulfuric acid and distilled.²⁴ Cyclohexane was purified by distillation prior to experiment; a 5.5 M solution of *tert*-butyl hydroperoxide in *n*-decane (SAF) was used without additional purification. NMR spectra were recorded on a Bruker Avance III 500 FT spectrometer. Signals in the ^1H and ^{13}C NMR spectra were assigned using 2D NMR spectroscopy (COSY, HMBC, and HSQC).

The kinetics of *tert*-butyl hydroperoxide decomposition in the presence and in the absence of clathrochelate $\text{FeBd}_2(\text{Cl}_2\text{Gm})(\text{BF})_2$ was measured by ^{13}C NMR spectroscopy.²¹ The solvents were 1,4-dioxane (0.3 mL), $\text{DMSO}-d_6$ (0.2 mL), and 5.5 M Bu^tOOH in *n*-decane (0.3 mL); $T = 100 \text{ }^\circ\text{C}$.

{1,8-Bis(2-fluorobora)-3,6,10,13,16,19-hexaaza-2,7,9,14,15,20-hexaoxa-17-chloro-4,5,11,12-tetraphenyl-18-cyclohexyl-bicyclo[6.6.6]eucosa-3,5,10,12,16,18-hexaene(2-)}iron(2+), $\text{FeBd}_2(\text{Cl}(\text{C}_6\text{H}_{11})\text{Gm})(\text{BF})_2$. Complex $\text{FeBd}_2(\text{Cl}_2\text{Gm})(\text{BF})_2$ (0.1 g, 0.135 mmol) was dissolved in benzene (30 mL), and the obtained solution was bubbled with argon for 3–4 min. Cyclohexane (2 mL) and a 5.5 M solution of *tert*-butyl hydroperoxide in *n*-decane (0.92 mL, 5 mmol) were added, and the reaction mixture was refluxed for 3 h. Next 72 h the reaction mixture was refluxed for 3.5, 3.5, and 4 h daily, adding three times a solution of *tert*-butyl hydroperoxide in *n*-decane (0.92 mL (5 mmol), 0.76 mL (4.18 mmol), and 0.8 mL (4.4 mmol), respectively). Then the reaction mixture was concentrated to dryness on a rotary evaporator, and the obtained oily residue was dried *in vacuo* and dissolved in chloroform. The chloroform extract was separated on a chromatographic column (1×20 cm, SiO_2 , CHCl_3 as eluent). The head fraction containing the target product was evaporated to dryness in air, and the solid residue was recrystallized from a dichloromethane—*n*-heptane (2 : 3) mixture. The yield was 0.064 g (60%). Found (%): C, 54.55; H, 4.16; N, 10.43; Fe, 7.10. $\text{C}_{36}\text{H}_{31}\text{N}_6\text{O}_6\text{B}_2\text{F}_2\text{ClFe}$. Calculated (%): C, 54.41; H, 3.93; N, 10.58; Fe, 7.03. ^1H NMR (CD_2Cl_2): 1.40 (m, 3 H, 3-H + 4-H_{Ch}); 1.78 (m, 1 H, 4-H_{Ch}); 1.83 (m, 2 H, 2-H_{Ch}); 1.91 (m, 2 H, 3-H_{Ch}); 2.19 (m, 2 H, 2-H_{Ch}); 3.52 (m, 1 H, 1-H_{Ch}); 7.3–7.45 (m, 20 H, Ph). $^{13}\text{C}\{^1\text{H}\}$ NMR (CD_2Cl_2): 25.91 (4-C_{Ch}); 26.65 (3-H_{Ch}); 28.12 (2-H_{Ch}); 40.29 (1-H_{Ch}); 128.42 (3-C_{Ph}); 129.47 (1-C_{Ph}); 130.66 (4-C_{Ph}); 130.95 (2-C_{Ph}); 132.86 (C_{Cl}=N); 157.13, 157.38 (PhC=N); 160.93 (ChC=N). ^{11}B NMR ($\text{BF}_3 \cdot \text{O}(\text{C}_2\text{H}_5)_2$): 3.6 (m). ^{19}F NMR (TFT, $\delta_{\text{CF}_3} = -63.73$): -169.29 (q), -169.48 (q). IR, ν/cm^{-1} : 929, 1060,

1105, 1159 (N—O), 1206 sh (B—O) + (B—F), 1360, 1444, 2853, 2926 (C—H).

X-ray diffraction study. Single crystals of complex $\text{FeBd}_2\text{-(Cl(C}_6\text{H}_{11}\text{)Gm)(BF)}_2\text{·CH}_2\text{Cl}_2$ suitable for X-ray diffraction analysis were obtained by the slow evaporation of a solution of the clathrocholate in a dichloromethane—hexane mixture.

The crystals of $\text{C}_{36}\text{H}_{31}\text{B}_2\text{ClF}_2\text{FeN}_6\text{O}_6\text{·CH}_2\text{Cl}_2$ are monoclinic at 150 K, space group $P2_1/c$, $a = 15.5803(7)$, $b = 14.8395(7)$, $c = 17.4961(5)$ Å, $\beta = 106.786(1)^\circ$, $V = 3872.8(3)$ Å³, $Z = 4$, $d_{\text{calc}} = 1.509$ g cm⁻³, $\mu = 0.611$ mm⁻¹. The intensities of 27 034 reflections were obtained on a Bruker Nonius X8 Apex diffractometer with a 4K CCD detector equipped with a graphite monochromator (Mo-K α radiation, $\lambda = 0.71073$ Å). An absorption correction was applied semiempirically based on the intensities of equivalent reflections.²⁵ The structure was solved by the direct method²⁶ and refined by full-matrix least squares against F^2 in the anisotropic approximation for non-hydrogen atoms using the SHELX97 program package.²⁷ Hydrogen atoms were geometrically localized and refined by the riding model. The dichloromethane molecule disordered over two positions was localized in structure refinement, and refinement of occupancies of these positions gave the ratio 0.45 : 0.55; these values were fixed in the final calculation. The refinement used 7818 independent reflections ($R_{\text{int}} = 0.048$). The refinement convergence for all independent reflections is $wR_2 = 0.1654$, GOOF = 1.019 ($R_1 = 0.0594$ for 4995 reflections with $I > 2\sigma$). When refining, mild restraints were imposed on the C—Cl bond lengths in the solvate dichloromethane molecule; the Cl—C—Cl bond angles were close to tetrahedral values and were refined without restraints. The thermal factors of the carbon atoms of the cyclohexyl substituent are increased, and their thermal ellipsoids are extended in the direction perpendicular to the root-mean-square plane of the cyclohexane ring and are larger for the atoms peripheral to the clathrocholate framework. The attempts to use different models of conformational disordering were unsuccessful. It is most likely that the increased thermal factors for the above mentioned carbon atoms are related to vibrations of the cyclohexyl substituent as a single whole. The obtained coordinates of atoms for complex $\text{FeBd}_2\text{(Cl(C}_6\text{H}_{11}\text{)Gm)(BF)}_2\text{·CH}_2\text{Cl}_2$ were deposited with the Cambridge Crystallographic Data Centre (CCDC 821653).

Quantum chemical calculations. The electronic structure of the clathrocholate precursor $\text{FeBd}_2\text{(Cl}_2\text{Gm)(BF)}_2$ and the 1,4-dioxanyl and cyclohexyl radicals were calculated using the DFT method in the ADF2010 program package.²⁸ The B3LYP hybrid functional was used as a density functional.²⁹ The basis sets consisted of triply split functions of the Slater type supplemented by the sets of polarization functions without the framework potential (TZP/ADF2010). The geometric parameters were optimized using the quasi-Newton method.³⁰ The optimization procedure of the geometric parameters showed that the studied radicals and clathrocholate $\text{FeBd}_2\text{(Cl}_2\text{Gm)(BF)}_2$ were in the bound states characterized by the positive calculated spectrum of vibrational modes indicating the ground state of the systems studied. The interatomic interactions were analyzed using the topological methods of quantum chemistry: by the electron density localization function (ELF)^{16,17} and the Bader theory (QTAIM).^{18,19} The ADFView program (grid 0.02 Å) was used for the visualization of the results of analysis of the electron density by the ELF method. The main calculated geometric parameters of the clathrocholate molecule agree qualitatively with the experimental data obtained by X-ray diffraction analysis (Table 1).

Table 1. Characteristic optimized and experimental (in parentheses) geometric parameters of the clathrocholate framework of the $\text{FeBd}_2\text{(Cl}_2\text{Gm)(BF)}_2$ molecule

Bond	$\delta/\text{\AA}$	Angle	ω/deg
Cl—C	1.720 (1.69)	N—Fe—N	79.4 (78)
C—N	1.296 (1.31)	N—C—C	113.5 (112)
N—O	1.345 (1.37)	N—O—B	112.5 (111)
O—B	1.507 (1.49)	Cl—C—C	122.9 (123)
N—Fe	1.954 (1.91)	F—B—O	107.7 (108)
B—F	1.357 (1.36)	O—N—C	118.8 (117)
C—C	1.455 (1.45)	Fe—N—C	116.5 (119)

This work was financially supported by the Russian Foundation for Basic Research (Project Nos 09-03-00540 and 10-03-00403). I. V. El'tsov is grateful to the Carl Zeiss AG for financial support.

References

1. Y. Z. Voloshin, N. A. Kostromina, R. Krämer, *Clathrocholates: Synthesis, Structure and Properties*, Elsevier, Amsterdam, 2002.
2. Y. Z. Voloshin, O. A. Varzatskii, T. E. Kron, V. K. Belsky, V. E. Zavodnik, A. V. Palchik, *Inorg. Chem.*, 2000, **39**, 1907.
3. Y. Z. Voloshin, V. E. Zavodnik, O. A. Varzatskii, V. K. Belsky, A. V. Palchik, N. G. Strizhakova, I. I. Vorontsov, M. Y. Antipin, *Dalton Trans.*, 2002, 1193.
4. Y. Z. Voloshin, O. A. Varzatskii, T. E. Kron, V. K. Belsky, V. E. Zavodnik, N. G. Strizhakova, V. A. Nadtochenko, V. A. Smirnov, *Dalton Trans.*, 2002, 1203.
5. Y. Z. Voloshin, O. A. Varzatskii, A. V. Palchik, I. I. Vorontsov, M. Y. Antipin, E. G. Lebed, *Inorg. Chim. Acta*, 2005, **358**, 131.
6. Y. Z. Voloshin, O. A. Varzatskii, A. V. Palchik, Z. A. Starikova, M. Y. Antipin, E. G. Lebed, Y. N. Bubnov, *Inorg. Chim. Acta*, 2006, **359**, 553.
7. Y. Z. Voloshin, O. A. Varzatskii, A. S. Belov, Z. A. Starikova, K. Y. Suponitsky, V. V. Novikov, Y. N. Bubnov, *Inorg. Chem.*, 2008, **47**, 2155.
8. Y. Z. Voloshin, O. A. Varzatskii, V. V. Novikov, N. G. Strizhakova, I. I. Vorontsov, A. V. Vologzhanina, K. A. Lysenko, G. V. Romanenko, M. V. Fedin, V. I. Ovcharenko, Y. N. Bubnov, *Eur. J. Inorg. Chem.*, 2010, 5401.
9. Y. Z. Voloshin, O. A. Varzatskii, A. S. Belov, Z. A. Starikova, A. V. Dolganov, V. V. Novikov, Y. N. Bubnov, *Inorg. Chim. Acta*, 2011, **370**, 322.
10. M. A. Vershinin, A. B. Burdakov, E. G. Boguslavskii, N. V. Pervukhina, N. V. Kuratieva, I. V. El'tsov, V. A. Reznikov, O. A. Varzatskii, Y. Z. Voloshin, Y. N. Bubnov, *Inorg. Chim. Acta*, 2011, **366**, 91.
11. A. Burdakov, M. Vershinin, I. El'tsov, N. Pervukhina, E. Boguslavskii, V. Reznikov, Y. Voloshin, *Proc. XVII Intern. Winter School Coord. Chem.*, Karpacz, Poland, 6–10 December 2010, 58.
12. M. A. Vershinin, A. B. Burdakov, I. V. El'tsov, V. A. Reznikov, E. G. Boguslavsky, Y. Z. Voloshin, *Polyhedron*, 2011, **30**, 1233.

13. H. Togo, *Advanced Free Radical Reactions for Organic Synthesis*, Elsevier, Amsterdam, 2004.
14. D. J. Pasto, *J. Org. Chem.*, 1992, **57**, 1139.
15. G. Zhang, C. B. Musgrave, *J. Phys. Chem. A*, 2007, **111**, 1554.
16. B. Silvi, A. Savin, *Nature*, 1994, **371**, 683.
17. J. Mellin, P. Fuentealba, *Intern. J. Quant. Chem.*, 2003, **92**, 381.
18. R. F. W. Bader, *Atoms in Molecules. A Quantum Theory*, Clarendon Press, Oxford, 1990.
19. I. S. Bushmarinov, K. A. Lysenko, M. Yu. Antipin, *Usp. Khim.*, 2009, **78**, 307 [*Russ. Chem. Rev., Int. Ed.*, 2009, **78**].
20. *Polymer Handbook*, 4th ed., Eds J. Brandrup, E. H. Immergut, E. A. Grulke, Vol. **1**, Wiley, 1998.
21. W. W. Fleming, S. A. MacDonald, *Anal. Chem.*, 1983, **55**, 1625.
22. H. B. Dunford, *Coord. Chem. Rev.*, 2002, **233–234**, 311.
23. Y. Z. Voloshin, V. E. Zavodnik, O. A. Varzatskii, V. K. Bel'sky, I. I. Vorontsov, M. Y. Antipin, *Inorg. Chim. Acta*, 2001, **321**, 116.
24. A. J. Gordon, R. A. Ford, *The Chemist's Companion*, Wiley—Interscience Public., New York, 1972.
25. Bruker AXS Inc. (2004), *APEX2* (Version 1.08), *SAINT* (Version 7.03), and *SADABS* (Version 2.11), Bruker Advanced X-ray Solutions, Madison, Wisconsin, USA.
26. M. C. Burla, R. Caliandro, M. Camalli, B. Carrozzini, G. L. Casciarano, L. De Caro, C. Giacovazzo, G. Polidori, R. Spagna, *J. Appl. Cryst.*, 2005, **38**, 381.
27. G. M. Sheldrick, *SHELXS97 and SHELX97. Programs for the Refinement of Crystal Structures*, University of Göttingen, Germany, 1997.
28. *Amsterdam Density Functional (ADF) Program*, Release 2006.02; Vrije Universiteit, Amsterdam, 2006.
29. P. J. Stephens, F. J. Devlin, C. F. Chabalowski, M. J. Frisch, *J. Phys. Chem.*, 1994, **98**, 11623.
30. L. Versluis, T. Ziegler, *J. Chem. Phys.*, 1988, **322**, 88.

Received June 22, 2011